et al. [17], Xu et al. [18] and Jun et al. [19] immobilized PEG derivatives on poly(acrylonitrile-*co*-maleic acid), polyurethane and Si(1 1 1), respectively. Groll et al. [20–22] prepared isocyanate-terminated star PEG for ultrathin coatings.

Existing immobilization strategies often require the presence of specific surface functional groups and extensive optimization, and they have a limited capacity to be used for modification of a variety of materials. Thus, there exists an ongoing need for versatile immobilization strategies that are capable of robustly anchoring PEG and other antifouling polymers onto a variety of medically relevant material surfaces. For this purpose, Dalsin et al. [23,24] employed a strategy using the adhesive characteristics of 3,4-dihydroxyphenylalanine, an important component of mussel adhesive proteins, to anchor PEG onto surfaces. On the other hand, Weber et al. [25] synthesized 1-aziglycoses, which are glycose-containing diazirines. Because of the low pK_a value and the expected weak nucleophilicity of the hydroxyl groups on the surface of oxidized titanium, 1-aziglycoses modified the titanium. The chemicals generated singlet carbenes that were readily inserted into H–O bonds, leading to the glycosidation of titanium. Photoimmobilization methods are also useful for universal anchoring.

We have employed a photoimmobilization technique, following that used by Matsuda and Sugawara [26], to immobilize growth factors [27], cytokines [28], sulfated hyaluronic acid [29], heparin [30], thermoresponsive polymer [31], β-galactose derivative [32], phosphatidylcholine derivative [33] and pullulan [34], and recently to microarray proteins and cells [35]. This photoimmobilization method is very useful because it is applicable to various materials. In addition, by using photolithography micropatterning, direct comparison between immobilized and non-immobilized surfaces is possible, resulting in the surface patterning of proteins and cells according to the properties of the micropatterned polymers. Although thin hydrogel formation by iniferter-based photopolymerization of dithiocarbamylated PEGs under UV irradiation or photopolymerization of monoacryloyl PEG has been reported by Lee et al. [36], Kwon and Matsuda [37] and Hahn et al. [38], surface modification by photocross-linking has not been reported.

In this study, PEG was chosen as a new material for photocross-linking immobilization on inorganic, organic and metal surfaces, and the subsequent interactions with proteins and cells was investigated. It was expected that the hydrated non-ionic surface would reduce interaction with biocomponents. Photocross-linking immobilization is generally useful in preparing micropatterned surfaces compared with the photopolymerization method, because the former uses a dry process.

2. Materials and methods

2.1. Materials

Polymethacryl–PEG with a molecular weight of about 360 was purchased from Aldrich, and used without further purification. Circular plates of plastic (Thermanox™, which is a polyester), 15 mm in diameter, were purchased from Nunc. Glass plate was purchased from Nikkyo Technos Co. Titanium-coated glass plate was prepared by sputtering of titanium (pressure, 2×10^{-5} Pa; gas, Ar) in Ulvac Inc. The bare and titan-coated glass plate was cleaned by VUV irradiation for 2 min.

2.2. Synthesis of acryloyl 4-azobenzene

Azidoaniline hydrochloride (500 mg, 2.9 mmol) was dissolved in MilliQ water (100 ml) and sodium carbonate (466 mg, 4.4 mmol) was added to the mixture to make the pH of solution 10. Methacryloyl chloride (460 mg, 4.4 mmol) in dioxane (10 ml) was added dropwise to the azidoaniline solution. Subsequently, the solution was allowed to stand for 2 h in the dark. After the reaction, the precipitate formed was recovered by filtration, washed with MilliQ water and dried (425 mg). The yield was 70.8% (57625-92-D). ^{1}H NMR (300 MHz, in $CDCl_3$), *d* (TMS, ppm): 7.56, 7.55 (dd, 2H, Bn-H), 7.50 (Br s, 1H, NH), 7.01, 6.98 (dd, 2H, Bn-H), 5.79, 5.48 (m, 2H, $=CH_2$), 2.06 (s, 3H CH_3).

2.3. Preparation of photoreactive PEG

Polymethacryl–PEG (3.4 g, 9.4 mmol) was mixed with acryloyl-4-azobenzene (100 mg, 0.5 mmol) and azobisisobutyronitrile (27.9 mg, 0.17 mmol) in ethanol (15 ml); the solution was bubbled with nitrogen gas for 20 min and then allowed to stand for 18 h at 60 °C. After removing the ethanol, the product was dialyzed with water and freeze dried. The yield was 2.7 g (78%). This copolymer is referred to as photoreactive PEG (Fig. 1).

2.4. Gel permeation chromatography and spectroscopic measurements

The photoreactive PEG was assayed by gel permeation chromatography (GPC) using TOSOH α-M column at 20 °C. Pure water (MilliQ water, pH 7.3) was used as an elution solvent. Detection was by using the refractive index. UV measurement was performed using a JASCO V-550 spectrophotometer.

2.5. Surface modification

Micropatterning was performed as follows. An aqueous solution of photoreactive PEG (0.1 wt.%) was cast on a substrate and air dried at room temperature. Subsequently, the plate was irradiated with UV light from a UV lamp (UV Spot Light Source L5662, Hamamatsu Photonics) at a distance of 5 cm for 10 s (16 mW cm^{-2}) with or without a photomask (Toppan Printing Co.). The plate was then repeatedly washed with distilled water.

The swelling ratio was determined as follows. The photoreactive PEG was cast on Thermanox™ and dried.

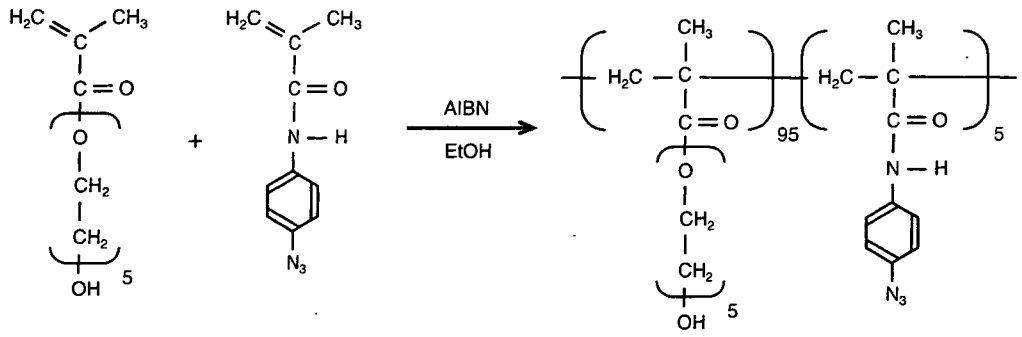

Fig. 1. Synthetic scheme for producing photoreactive PEG.

Subsequently the dried plate was photoirradiated. The plate was then incubated in water and the weight change measured.

2.6. Surface characterization

Contact angle measurement was performed as previously reported [30]. The unpatterned sample was placed on the stage of a CA-W Automatic Contact Angle Meter (Kyowa Interface Co. Ltd.) and a drop of water (0.1 μl) was put on the sample surface. The contact angle of the drop on the surface was measured at room temperature. At least 10 angles were measured at different areas and averaged.

Measurement of time-of-flight secondary ion mass spectrometry (TOF-SIMS) was carried out by using a TFS-2000 (Physical Electronics). The primary ion was $^{69}Ga^{+}$; the accelerating voltage of the ion gun was 25 kV, the pulse width 12 ns, the pulse frequency 8.3 kHz, the range of mass 0–1000 amu and the resolution of time 1.1 ns ch^{-1}.

Atomic force microscopic (AFM) observation was performed using a Nanoscope IV (Digital Instruments Inc.). The micropatterned sample was set in a cell holder into which water could be injected. After observation of the dry sample, distilled water was injected into the sample cell and the same position was observed. The measurement was performed using the tapping mode with a nominal force constant of 0.09 N m^{-1}.

2.7. Protein adsorption

Polyclonal rabbit anti-mouse antibodies conjugated with horseradish peroxidase (HRP-IgG) were purchased from Dako Cytomation and used as representative proteins. The plates were soaked in the protein solution (0.5 mol ml^{-1} diluted in phosphate-buffered saline (PBS)) for 30 min at 37 °C, then washed sequentially with PBS and distilled water. Adsorbed proteins were detected by HRP activity. A 3,3,5,5-tetramethyl benzidine (TMB) peroxidase substrate kit was purchased from Vector Laboratories and used to stain the plates. The blue staining of TMB was observed by phase-contrast microscopy.

HRP-conjugated bovine serum albumin (HRP–BSA, purchased from Rockland) was also used for an adsorption experiment. A 3 μl aliquot of HRP–BSA (50 and 100 ng ml^{-1}) was added to the samples and allowed to stand for 1 h. After washing with PBS, the chemiluminescence from the sample surface was measured using an ECL Advance Western blotting detection kit purchased from Amersham Bioscience. Calibration was performed using HRP–BSA solutions of known concentrations.

2.8. Cell culture

COS-7 cells with epithelial cell morphology growing as monolayers and African green monkey kidney derived from CV-1, a simian cell line (*Cercopithecus aethiops*), were purchased from the Riken Cell Bank and cultured in Dulbecco's modified Eagle's medium (Sigma) containing 10% fetal bovine serum. The cultured cells were recovered by treatment with PBS containing 0.25 wt.% trypsin and 0.9 mM ethylenediaminetetraacetic acid. The recovered cells were washed with the culture medium and finally suspended in this medium (1.8×10^5 cells per well of a 12-well plate). The cell suspension was added to sample plates, which had been sterilized with 70% ethanol. The cells were incubated at 37 °C under 5% v/v of CO_2 for 19 h, and were observed by phase-contrast microscopy.

3. Results and discussion

3.1. Synthesis of photoreactive PEG

GPC chromatograms of photoreactive PEG are shown in Fig. 2. A significant increase of molecular weight was observed for the photoreactive PEG. Its molecular weight was estimated to be around 8100, after calibration with polyethylene glycol standards.

The UV spectrum of photoreactive PEG is shown in Fig. 3. Absorption at 276 nm, attributable to the azidophenyl group, was observed. The absorption was red shifted by 20 nm from the corresponding absorption of 4-azidoaniline. This shift may be due to electron delocalization of the azidophenyl group caused by amide bond formation. In previous studies, the peaks of photoreac-

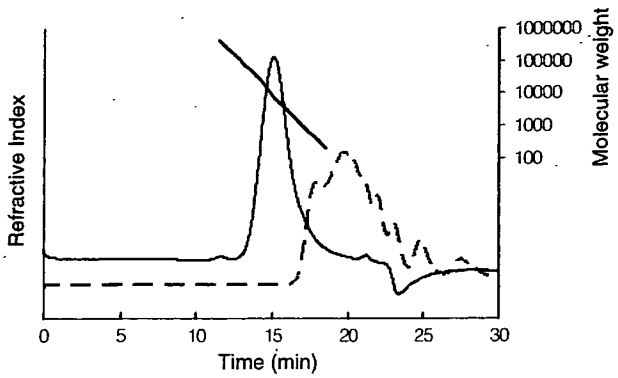

Fig. 2. Gel permeation chromatography of polymethacryl–PEG (broken line) and photoreactive PEG (solid line).

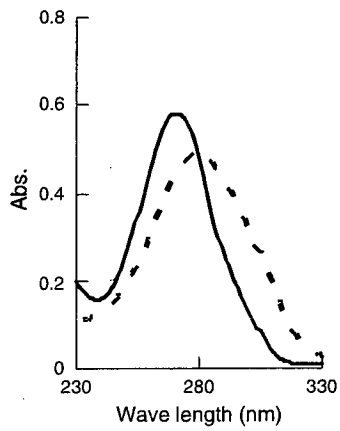

Fig. 3. UV spectrum of 4-azidoaniline hydrochloride (9.2 μg ml^{-1}, broken line) and photoreactive PEG (0.1 wt.% (the content of azidophenyl groups is 10.5 μg ml^{-1}), solid line).

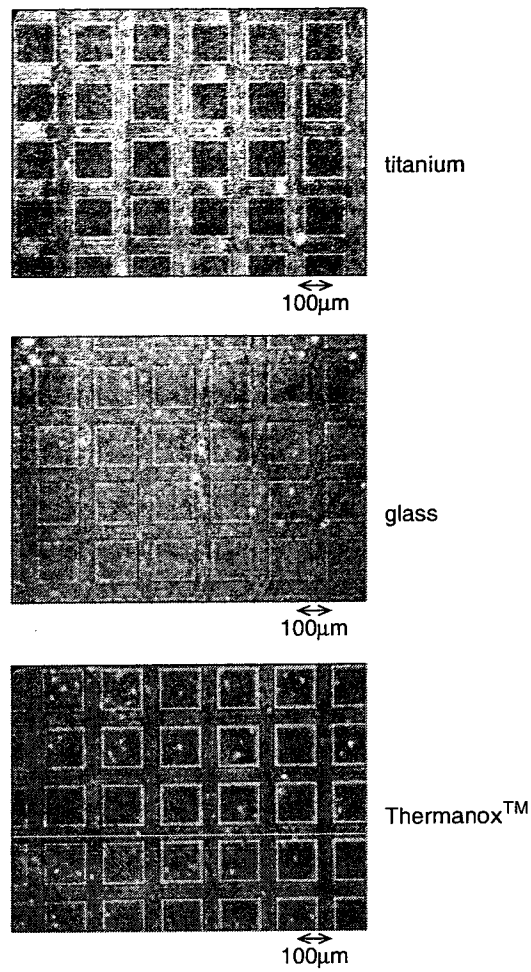

Fig. 4. Phase-contrast micrographs of micropatterned titanium, glass and Thermanox™ surfaces.

tive gelatin, hyaluronic acid, and heparin were also red shifted from azidobenzoic acid [28–30]. However, the shifted wavelength was the highest among the photoreactive biopolymers.

Assuming that the molecular absorption coefficient of the azidophenyl group at 276 nm was the same as that of azidoaniline at 256 nm, the content of azidophenyl groups in the photoreactive PEG was calculated to be 3.3 wt.%.

3.2. Photoimmobilization

Photoreactive PEG was coated onto the glass, titanium and plastic plates, and the coated surface was UV-irradiated in the presence of a photomask (Fig. 4). The wet polymer contained 76 ± 2% water. The micropatterns on three types of surfaces were identical to that of the photomask. This demonstrated that the surfaces could be modified by photoreactive PEG. The cast photoreactive PEG formed intra- and intermolecular networks and bonded with the surfaces because of the presence of these radical groups.

The micropattern was also confirmed by TOF-SIMS. In the spectrum of positive secondary ion, peaks of $^{31}CH_3O^+$, $^{45}C_2H_5O^+$, $^{59}C_3H_7O^-$ and $^{89}C_4H_9O_2^+$, which were attributed to organic materials, were observed. In the spectrum of negative secondary ions, peaks of $^{43}C_2H_3O^-$, $^{55}C_3H_3O^-$, $^{59}C_2H_5O_2^-$ and $^{85}C_4H_5O_2^-$, which were attributed to organic materials, were observed. These fragments were observed in the lattices on titanium, glass and plastic surfaces as the $C_2H_5O^+$ ion image of Fig. 5. No signal of organic materials between the lattices of titanium surfaces was detected. Because Thermanox™ is a polyester, there are some signals of $C_2H_5O^+$. However, the intensity from immobilized PEG was higher than on non-immobilized areas. On glass surfaces, the contrast was between titanium and Thermanox™. On the other hand, there were no signals of PEG detected from the areas non-irradiated on titan, glass and Thermanox™, by Ti^+, $Si_2O_5H^-$ and $C_7H_4O^+$, respectively. This result shows the formation of defect-free PEG layers.

In addition, the thickness of the micropattern-immobilized PEG was investigated by AFM, as shown in Fig. 6.

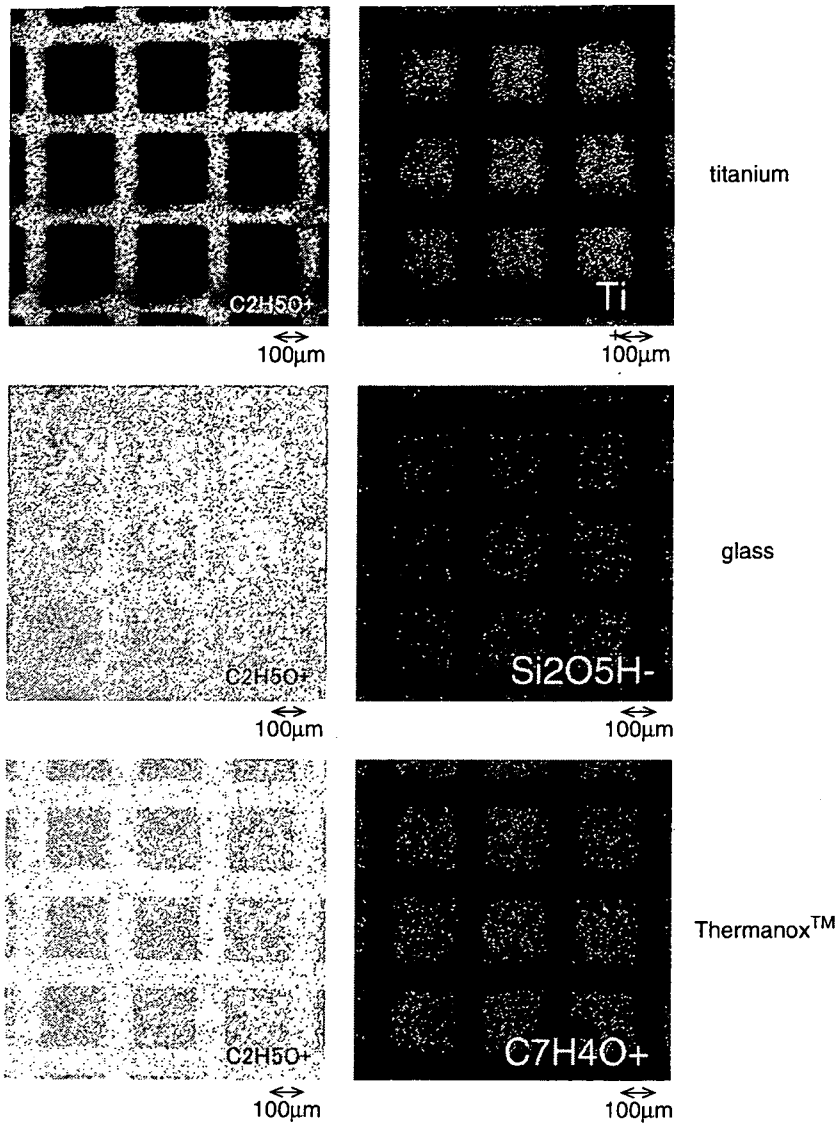

Fig. 5. TOF-SIMS image of PEG-micropatterned titanium, glass and Thermanox™.

The thickness (several hundred nanometers) was similar to that formed by the same amount of other photoreactive polymers that we prepared [33,39].

The surface properties of the immobilized photoreactive PEG without using a photomask were investigated by contact angle measurements, as shown in Table 1. Although the original polymer or modified glass had different contact angles, the photoreactive PEG-immobilized surfaces had almost the same contact angle. These results indicated that the surfaces were completely covered using the photoimmobilization method.

Photoimmobilization of photoreactive polymers on plastic materials has been previously reported [26–31, 33–35]. The phenyazide groups in the photoreactive polymers were photolyzed to generate highly reactive nitrene, which spontaneously formed intra- and intermolecularly bonds with neighboring organic materials.

Weber et al. [25] synthesized 1-aziglycoses, which are glycose-containing diazirines. Because of the low pK_a value and the expected weak nucleophilicity of the hydroxyl groups on the surface of oxidized titanium, 1-aziglycoses were used to modify the titanium. Although they did not show any evidence for a direct bond between the glucose and titanium, it was considered that the chemicals generated singlet carbenes that were readily inserted into H–O bonds, leading to the glycosidation of titanium. Considering that the concentration of photoreactive groups is very low and that bonds will be formed only at the surface of the substrate, it is very difficult to detect the bonds. Recently Adden et al. [40] developed a bifunctional copolymer of (4-vinylbenzyl)phosphoric acid diethylester and *N*-acryloxysuccinimide that is bound to a titanium surface. However, they detected no direct chemical bond between the phosphoric acid and titanium by XPS.

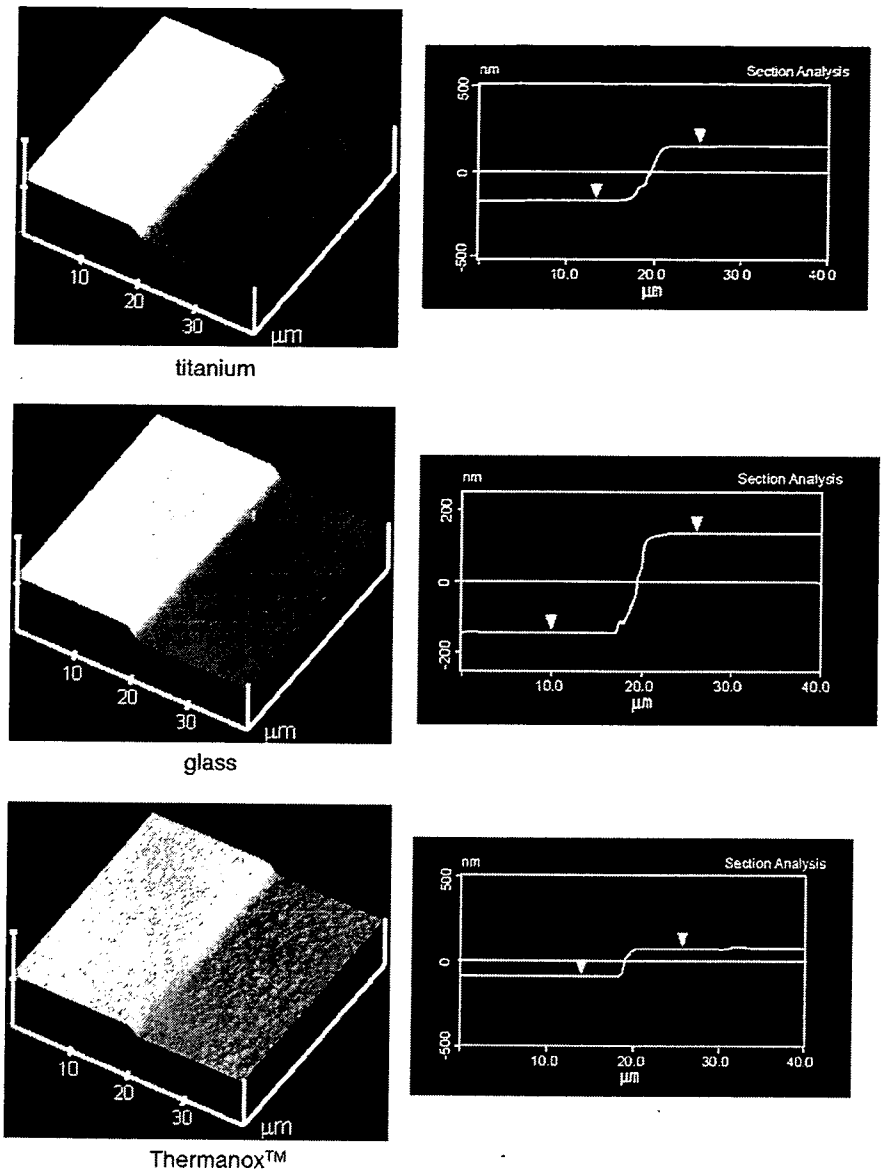

Fig. 6. AFM images of PEG micropatterned on titanium, glass and Themanox™.

Table 1
Contact angles on surfaces

Surface	Contact angle (°)
Titanium	0[a]
Titanium with photoreactively immobilized PEG	39.2 ± 1.3
Glass	6.4 ± 1.2
Glass with photoreactively immobilized PEG	40.9 ± 0.7
Thermanox™	78.8 ± 0.7
Thermanox™ with photoreactively immobilized PEG	41.0 ± 2.7

[a] The value was reported in a previous report [44].

Therefore, we performed micropatterning. If a micropattern was formed, we considered that photoimmobilization occurred. Without photoirradiation, no PEG was found by TOF-SIMS and AFM on the surface where there was no irradiation. It was considered that aryl azide derivatives form short-lived nitrenes that react extremely rapidly with the surrounding chemical environment [41]. Recent evidence, however, indicates that photolyzed intermediates of aryl azides can undergo ring expansion to create nucleophile-reactive dehydroazepines [41].

3.3. Protein adsorption

To assess the non-specific adsorption of protein on immobilized PEG surfaces, micropatterned plates of titanium-coated glass, glass and plastics were soaked in HRP-conjugated antibody solution. Adsorbed proteins

were detected by their HRP activity. Blue staining by HRP substrates was clearly observed on the non-PEG immobilized region of each surface and the staining was vanishingly small on the PEG photoimmobilized regions, as shown in Fig. 7.

Protein adsorption was investigated using another protein, albumin (BSA), which is smaller than the antibody and the amount of adsorbed protein was quantitatively determined. As shown in Fig. 8a, the adsorption was significantly reduced by the immobilization of PEG. The reduction effect is quantitatively evaluated and shown in Fig. 8b.

3.4. Cell adhesion

Adhesion of COS-7 cells on the micropatterned surfaces is shown in Fig. 9. Taking into consideration previous reports, an incubation time of 19 h was considered sufficient to allow comparison of the immobilized PEG and uncoated surfaces [42,43]. No cell adhesion was observed on the PEG-immobilized regions. It is known that COS-7 cells have epithelial cell properties and adhere to various materials [42,43]. However, immobilized PEG inhibited the adhesion of these very sticky cells. As the PEG-immobilized surface formed a hydrophilic diffused layer, it was thus considered to reduce cell adhesion, as do conventional hydrogel surfaces, which also reduce interactions with cells [33,34]. Employment of photoreactive PEG is therefore considered a new method for the preparation of bioinert surfaces, as it can reduce interactions with biological proteins and cells.

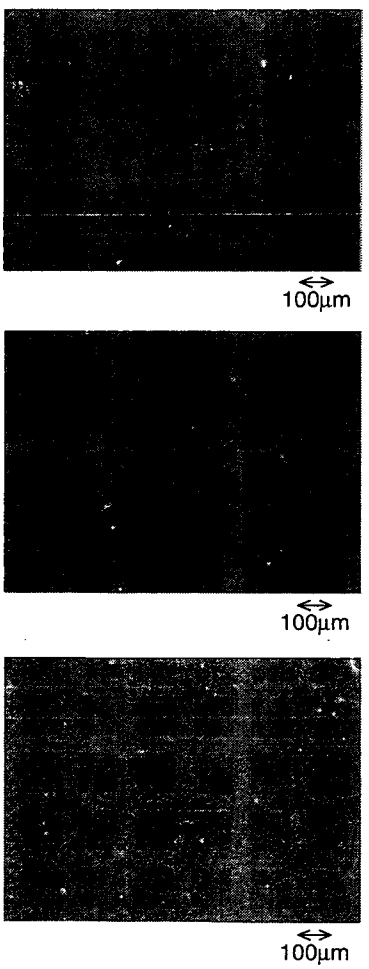

Fig. 7. Protein adsorption using HRP-IgG on PEG-micropatterned titanium, glass, and Thermanox™.

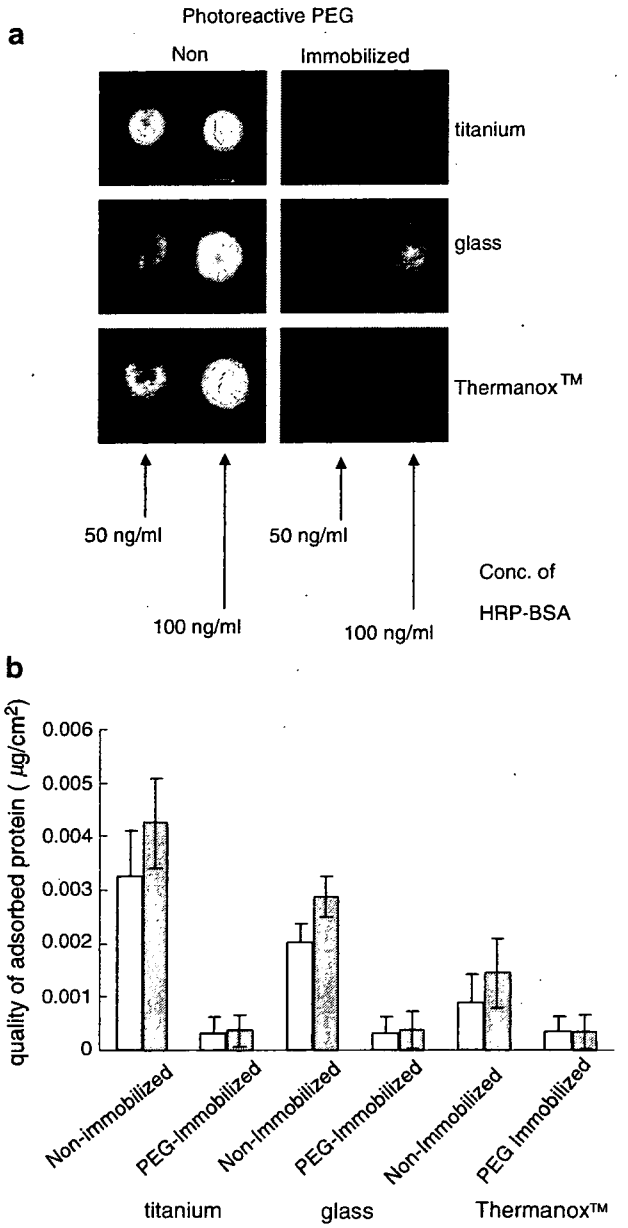

Fig. 8. (a) Chemiluminescence of HRP–BSA on non-immobilized and PEG-photoimmobilized titanium, glass, and Thermonox™. (b) The amount of HRP–BSA on non-immobilized and PEG-photoimmobilized titanium, glass, and Thermonox™. Open and closed columns indicate 50 and 100 ng ml^{-1} of protein concentrations, respectively.

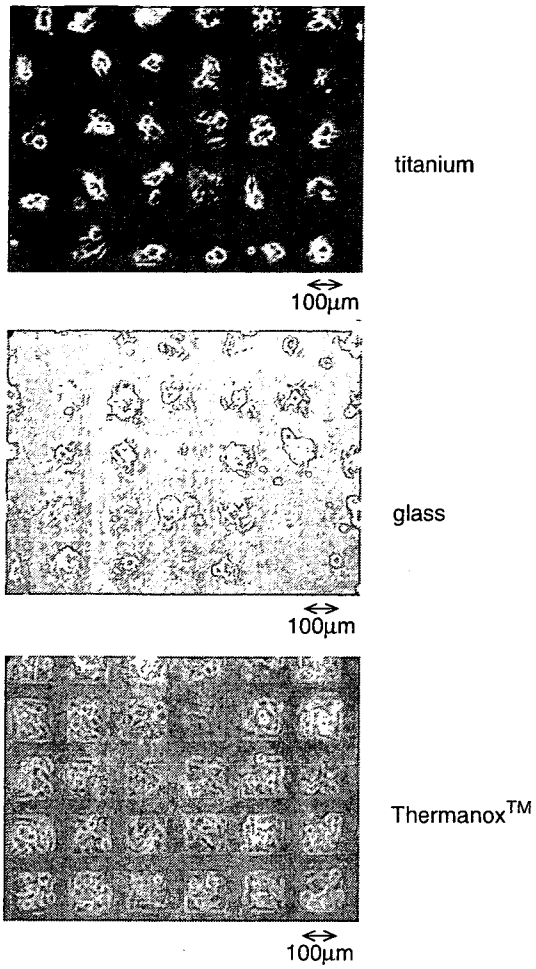

Fig. 9. Adhesion of COS-7 cells on micropattern photoimmobilized PEG on titanium, glass and Thermanox™.

4. Conclusions

This study demonstrated photoimmobilization of PEG onto various types of surfaces, including metal, glass and plastics. The immobilization technique is very useful for surface modification because of its convenience. In addition, micropatterning was achieved by the immobilization technique. The modified surface significantly reduced the interaction with proteins. In addition, the modified surface stably reduced cell adhesion in culture.

References

[1] Ratner BD, Hoffman AS. Nonfouling surfaces. In: Ratner BD, Hoffman AS, Schoen FJ, Lemons JE, editors. Biomaterials science. 2nd ed. San Diego, CA: Elsevier Academic Press; 2004. p. 197–201.
[2] Rundqvist J, Hoh JH, Haviland DB. Directed immobilization of protein-coated nanospheres to nanometer-scale patterns fabricated by electron beam lithography of poly(ethylene glycol) self-assembled monolayers. Langmuir 2006;22:5100–7.
[3] Mougin K, Ham AS, Lawrence MB, Fernandez EJ, Hillier AC. Construction of a tethered poly(ethylene glycol) surface gradient for studies of cell adhesion kinetics. Langmuir 2005;21:4809–12.
[4] Sebra RP, Masters KS, Cheung CY, Bowman CN, Anseth KS. Detection of antigens in biologically complex fluids with photografted whole antibodies. Anal Chem 2006;78:3144–51.
[5] Ko YG, Kim YH, Park KD, Lee HJ, Lee WK, Park HD, et al. Immobilization of poly(ethylene glycol) or its sulfonate onto polymer surfaces by ozone oxidation. Biomaterials 2001;22:2115–23.
[6] Beyer M, Felgenhauer T, Bischoff FR, Breitling F, Stadler V. A novel glass slide-based peptide array support with high functionality resisting non-specific protein adsorption. Biomaterials 2006;27:3505–14.
[7] Kızılel S, Sawardecker E, Teymour F, Pérez-Luna VH. Sequential formation of covalently bonded hydrogel multilayers through surface initiated photopolymerization. Biomaterials 2006;27:1209–15.
[8] Sun XL, Stabler CL, Cazalis CS, Chaikof EL. Carbohydrate and protein immobilization onto solid surfaces by sequential Diels–Alder and azide–alkyne cycloadditions. Bioconj Chem 2006;17:52–7.
[9] Schlapak R, Pammer P, Armitage D, Zhu R, Hinterdorfer P, Vaupel M, et al. Glass surfaces grafted with high-density poly(ethylene glycol) as substrates for DNA oligonucleotide microarrays. Langmuir 2006;22:277–85.
[10] Feng CL, Zhang Z, Forch R, Knoll W, Vancso GJ, Schonherr H. Reactive thin polymer films as platforms for the immobilization of biomolecules. Biomacromolecules 2005;6:3243–51.
[11] Patel S, Thakar RG, Wong J, McLeod SD, Li S. Control of cell adhesion on poly(methyl methacrylate). Biomaterials 2006;27:2890–7.
[12] Sinclair J, Salem AK. Rapid localized cell trapping on biodegradable polymers using cell surface derivatization and microfluidic networking. Biomaterials 2006;27:2090–4.
[13] Zhen G, Eggli V, Voros J, Zammaretti P, Textor M, Glockshuber R, et al. Immobilization of the enzyme beta-lactamase on biotin-derivatized poly(L-lysine)-*g*-poly(ethylene glycol)-coated sensor chips: a study on oriented attachment and surface activity by enzyme kinetics and in situ optical sensing. Langmuir 2004;20:10464–73.
[14] Popat KC, Mor G, Grimes CA, Desai TA. Surface modification of nanoporous alumina surfaces with poly(ethylene glycol). Langmuir 2004;20:8035–41.
[15] Piehler J, Brecht A, Valiokas R, Liedberg B, Gauglitz G. A high-density poly(ethylene glycol) polymer brush for immobilization on glass-type surfaces. Biosens Bioelectron 2000;15:473–81.
[16] Xu ZK, Nie FQ, Qu C, Wan LS, Wu J, Yao K. Tethering poly(ethylene glycol)s to improve the surface biocompatibility of poly(acrylonitrile-*co*-maleic acid) asymmetric membranes. Biomaterials 2005;26:589–98.
[17] Choi I, Kang SK, Lee J, Kim Y, Yi J. In situ observation of biomolecules patterned on a PEG-modified Si surface by scanning probe lithography. Biomaterials 2006;27:4655–60.
[18] Xu H, Kaar JL, Russell AJ, Wagner WR. Characterizing the modification of surface proteins with poly(ethylene glycol) to interrupt platelet adhesion. Biomaterials 2006;27:3125–35.
[19] Jun Y, Cha T, Guo A, Zhu XY. Patterning protein molecules on poly(ethylene glycol) coated Si(1 1 1). Biomaterials 2004;25:3503–9.
[20] Groll J, Ameringer T, Spatz JP, Moeller M. Ultrathin coatings from isocyanate terminated star PEG prepolymers: layer formation and characterization. Langmuir 2005;21:1991–9.
[21] Groll J, Haubensak W, Ameringer T, Moeller M. Ultrathin coatings from isocyanate terminated star PEG prepolymers: patterning of proteins on the layers. Langmuir 2005;21:3076–83.
[22] Groll J, Ademovic Z, Ameringer T, Klee D, Moeller M. Comparison of coatings from reactive star shaped PEG-stat-PPG prepolymers and grafted linear PEG for biological and medical applications. Biomacromolecules 2005;6:956–62.
[23] Dalsin JL, Lin L, Tosatti S, Vörös J, Textor M, Messersmith PB. Protein resistance of titanium oxide surfaces modified by biologically inspired mPEG-DOPA. Langmuir 2005;21:640–6.
[24] Dalsin JL, Hu B-H, Lee BP, Messersmith PB. Mussel adhesive protein mimetic polymers for the preparation of nonfouling surfaces. J Am Chem Soc 2003;125:4253–8.

[25] Weber M, Vasella A, Textor M, Spencer ND. Glycosydene carbenes: Part 271. Glucosidation of titanium dioxide with 1-aziglucoses: preparation and characterization of modified titanium-dioxide E surface. Helv Chim Acta 1998;81:1359–72.
[26] Sugawara T, Matsuda T. Photochemical protein fixation on polymer surfaces via derivatized phenyl azido group. Langmuir 1995;11:2272–6.
[27] Chen G, Ito Y. Gradient micropattern immobilization of EGF to investigate the effect of artificial juxtacrine stimulation. Biomaterials 2001;22:2453–7.
[28] Ito Y, Hasuda H, Yamauchi T, Komatsu N, Ikebuchi K. Immobilization of erythropoietin to culture erythropoietin-dependent human leukemia cell line. Biomaterials 2004;25:2293–8.
[29] Chen G, Ito Y, Imanishi Y, Magnani A, Lamponi S, Barbucci R. Photoimmobilization of sulfated hyaluronic acid for antithrombogenicity. Bioconjugate Chem 1997;8:730–4.
[30] Ito Y, Hayashi M, Imanishi Y. Gradient micropattern immobilization of heparin and its interaction with cells. J Biomater Sci Polym Edn 2001;12:367–78.
[31] Liu H, Ito Y. Gradient micropattern immobilization of a thermoresponsive polymer to investigate its effect on cell behavior. J Biomed Mater Res 2003;67A:1424–9.
[32] Kang I-K, Kim GJ, Kwon OH, Ito Y. Co-culture of hepatocytes and fibroblasts by micropatterned immobilization of beta-galactose derivatives. Biomaterials 2004;25:4225–32.
[33] Konno T, Hasuda H, Ishihara K, Ito Y. Photo-immobilization of a phospholipid polymer for surface modification. Biomaterials 2005;26:1381–8.
[34] Hasuda H, Kwon OH, Kang I-K, Ito Y. Synthesis of photoreactive pullulan for surface modification. Biomaterials 2005;26:2401–6.
[35] Ito Y. Photoimmobilization for microarrays. Biotechnol Prog 2006;22:924–32.
[36] Lee BP, Huang K, Nunalee FN, Shull KR, Messersmith PB. Synthesis of 3,4-dihydroxyphenylalanine (DOPA) containing monomers and their co-polymerization with PEG-diacrylate to form hydrogels. J Biomater Sci Polym Edn 2004;15:449–64.
[37] Kwon IK, Matsuda T. Photo-iniferter-based thermoresponsive block copolymers composed of poly(ethylene glycol) and poly(*N*-isopropylacrylamide) and chondrocyte immobilization. Biomaterials 2006;27:986–95.
[38] Hahn MS, Taite LJ, Moon JJ, Rowland MC, Ruffino KA, West JL. Photolithographic patterning of polyethylene glycol hydrogels. Biomaterials 2006;27:2519–24.
[39] Chen G, Imanishi Y, Ito Y. pH-Sensitive thin hydrogel microfabricated by photolithography. Langmuir 1998;14:6610–2.
[40] Adden N, Gamble LJ, Castner DG, Hoffman A, Cross G, Menzel H. Synthesis and characterization of biocompatible polymer interlayers on titanium implant materials. Biomacromolecules 2006;7:2552–9.
[41] Hermanson GH. Bioconjugate techniques. Academic Press; 1996.
[42] Ito Y, Nogawa M. Preparation of a protein micro-array using a photo-reactive polymer for a cell-adhesion assay. Biomaterials 2003;24:3021–6.
[43] Ito Y, Nogawa M, Takeda M, Shibuya T. Photo-reactive polyvinylalcohol for photo-immobilized microarray. Biomaterials 2005;26:211–6.
[44] Heydari M, Hasuda H, Sakuragi M, Yoshida Y, Suzuki K, Ito Y. Modification of the titan surface with photoreactive gelatin to regulate cell attachment. J Biomed Mater Res; in press. doi:10.1002/jbm.a.31368.

Grid Pattern of Nanothick Microgel Network

Guoping Chen,*,† Naoki Kawazoe,† Yujiang Fan,†,§ Yoshihiro Ito,‡ and Tetsuya Tateishi†

Biomaterials Center, National Institute for Materials Science, 1-1 Namiki, Tsukuba, Ibaraki 305-0044, Japan and Nano Medical Engineering Laboratory, Institute of Physical and Chemical Research, 2-1 Hirosawa, Wako, Saitama 351-0198, Japan

Received March 31, 2007

A novel grid pattern of two kinds of nanothick microgels was developed by alternate patterning using photolithography. At first, 100-μm-wide nanothick PAAm microgel stripes were grafted on a polystyrene surface by UV irradiation of the photoreactive azidobenzoyl-derivatized polyallylamine-coated surface through a photomask with 100-μm-wide stripes. Then, a second set of 100-μm-wide nanothick PAAc microgel stripes were grafted across the PAAm-grated polystyrene surface by UV irradiation of the photoreactive azidophenyl-derivatized poly(acrylic acid)-coated surface through a photomask placed perpendicularly to the first set of PAAm microgel stripes. The PAAc microgel stripe pattern was formed over the PAAm microgel stripe pattern. The cross angle of the two microgel stripes could be controlled by adjusting the position of the photomask when the second microgel pattern was prepared. Swelling and shrinking of the microgels were investigated by scanning probe microscopy (SPM) in an aqueous solution. SPM observation indicated that the thickness of the gel network was 100 to 500 nm. The regions containing PAAm, PAAc, and the PAAc-PAAm overlapping microgels showed different swelling and shrinking properties when the pH was changed. The PAAm microgel swelled at low pH and shrank at high pH whereas the PAAc microgel swelled at high pH and shrank at low pH. However, the PAAc-PAAm overlapping microgel did not change as significantly as did the two microgels, indicating that the swelling and shrinking of the two gels was partially offset. The pH-induced structural change was repeatedly reversible. The novel grid pattern of nanothick microgels will find applications in various fields such as smart actuators, artificial muscles, sensors, and drug delivery systems as well as in tissue engineering and so forth.

Introduction

Intelligent hydrogel systems have many potential applications because they undergo huge changes in volume in response to external stimuli such as changes in solvent composition,[1] pH,[2] temperature,[3] ion concentration,[4] electric field,[5] and light irradiation.[6] Some systems respond to a combination of two or more stimuli.[7,8] They have been used in actuators,[9] sensors,[10] drug delivery systems,[11] bioseparations,[12] biomedicine,[13] cell culture, and tissue engineering.[14,15] Many studies have focused on the response and structure of hydrogels. Their sensitivity can be controlled by molecular design technologies.[16−18] To accelerate the swelling and shrinking of hydrogels, efforts have been made to introduce porosity into hydrogels[19] or to reduce the size of hydrogels such as synthesizing microgels.[20,21] However, there are no reports on controlling the network pattern of different microhydrogels. In this study, an alternate patterning technique was developed to influence the network pattern of microgels. Photolithography was used to prepare a novel grid pattern of two different nanothick microgels. The pH responses of the microgel networks were observed by scanning probe microscopy (SPM). The grid patterns consisted of poly(acrylic acid), polyallylamine, and overlapping poly(acrylic acid)-on-polyallylamine microgel areas that demonstrated different pH responses.

Experimental Section

Synthesis of Azidophenyl-Derivatized Poly(acrylic acid). Azidophenyl-derivatized poly(acrylic acid) conjugate was synthesized by coupling poly(acrylic acid) with 4-azidoaniline. Poly(acrylic acid) (MW 450 000, 1.0 mmol per monomer unit), 4-azidoaniline hydrochloride (0.1 mmol), and 1-ethyl-3-(3-(dimethylamino)propyl) carbodiimide (water-soluble carbodiimide, WSC, 6.0 mmol) were dissolved in deionized water (110 mL). The pH of the solution was adjusted to 7.0 by adding NaOH and HCl. After being stirred at 4 °C for 48 h, the reaction solution was dialyzed against MilliQ water through a seamless cellulose tube (cutoff molecular weight 12 000) until the absence of azidoaniline in the washing solution was confirmed by ultraviolet spectroscopy. The dialyzed polymer was freeze dried. The azidophenyl-derivatized poly(acrylic acid) was

* To whom correspondence may be addressed. E-mail: guoping.chen@nims.go.jp. Tel: +81-29-860-4496. Fax: +81-29-860-4715.
† National Institute for Materials Science.
‡ Institute of Physical and Chemical Research.
§ Current affiliation: National Engineering Research Center for Biomaterials, Sichuan University, 29 Wangjiang Road, Chengdu 610064, China.

(1) Tanaka, T.; Fillmore, D.; Sun, S. T.; Nishio, I.; Swislow, G.; Shah, A. *Phys. Rev. Lett.* **1980**, *45*, 1636−1639.
(2) Zhao, B.; Moore, J. S. *Langmuir* **2001**, *17*, 4748−4763.
(3) Wang, C.; Stewart, R. J.; Kopecek, J. *Nature* **1999**, *397*, 417−420.
(4) Holz, J. H.; Holz, J. S.; Munro, C. H.; Asher, S. A. *Anal. Chem.* **1998**, *70*, 780−781.
(5) Osada, Y.; Okuzaki, H.; Hori, H. *Nature* **1992**, *355*, 242−243.
(6) Suzuki, A.; Tanaka, T. *Nature* **1992**, *346*, 345−346.
(7) Sahoo, S. K.; De, T. K.; Ghosh, P. K.; Maitra, A. *J. Colloid Interface Sci.* **1998**, *206*, 361−368.
(8) Kim, S. J.; Spinks, G. M.; Prosser, S.; Whitten, P. G.; Wallace, G. G.; Kim, S. I. *Nat. Mater.* **2006**, *5*, 48−51.
(9) Beebe, D. J.; Moore, S. J.; Bauer, J. M.; Yu, Q.; Liu, H. *Nature* **2000**, *404*, 588−590.
(10) Byrne, M. E.; Park, K.; Peppas, N. A. *Adv. Drug Delivery Rev.* **2002**, *54*, 149−161.
(11) Guiseppi-Elie, A.; Brahim, S. I.; Narinesingh, D. *Adv. Mater.* **2002**, *14*, 743−746.
(12) Galaev, I. Y.; Mattiasson, B. *TIBTECH* **1999**, *17*, 335−340.
(13) Hoffman, A. S. *Adv. Drug Delivery Rev.* **2002**, *43*, 3−12.
(14) Alsberg, E.; Anderson, K. W.; Albeiruti, A.; Rowley, J. A.; Mooney, D. J. *Proc. Natl. Acad. Sci. U.S.A.* **2002**, *99*, 12025−12030.
(15) Stabenfeldt, S. E.; Garcia, A. J.; LaPlaca, M. C. *J. Biomed. Mater. Res., Part A* **2006**, *77*, 718−725.
(16) Yoshida, R.; Uchida, K.; Kaneko, Y.; Sakai, K.; Kikuchi, A.; Sakurai, Y.; Okano, T. *Nature* **1995**, *374*, 240−242.
(17) Chen, G.; Hoffman, A. S. *Nature* **1995**, *373*, 49−51.
(18) Yoshida, R.; Takahashi, T.; Yamaguchi, T.; Ichijo, H. *Adv. Mater.* **1997**, *9*, 175−178.
(19) Barbucci, R.; Leone, G.; Vecchiullo, A. *J. Biomater. Sci., Polym. Ed.* **2004**, *15*, 607−619.
(20) Wang, J.; Gan, D.; Lyon, L. A.; El-Sayed, M. A. *J. Am. Chem. Soc.* **2001**, *123*, 11284−11289.
(21) Chen, G.; Imanishi, Y.; Ito, Y. *Macromolecules* **1998**, *31*, 4379−4381.

10.1021/la700931u CCC: $37.00
Published on Web 04/26/2007

referred to as AzPhPAAc. The number of azidophenyl groups in the polymer was determined by ^{1}H NMR from the peak intensities of the azidophenyl protons at 7.0 ppm and those of the methylene and methylidyne protons of the polymer main chain at 1.3 and 2.5 ppm.

Preparation of Azidophenyl-Derivatized Polyallylamine. *N*-(4-Azidobenzoyloxy) succinimide was at first synthesized. A solution of DCC (13.3 g, 64.6 mmol) in tetrahydrofuran (THF 50 mL) was added dropwise to a solution of *N*-hydroxysuccinimide (7.43 g, 64.6 mmol) and 4-azidobenzoic acid (9.57 g, 58.7 mmol) in 150 mL of THF in an ice bath under stirring. After 3 h, the reaction mixture was slowly warmed to room temperature, and stirring was continued overnight. The white solid that formed was filtered off, and the solvent was removed under reduced pressure. The remaining yellow residue was crystallized from isopropyl alcohol/isopropyl ether. Then the azidophenyl-derivatized polyallylamine conjugate was synthesized by coupling polyallylamine with *N*-(4-azidobenzoyloxy) succinimide. An aqueous solution (pH 7.0, 10 mL) containing polyallylamine (MW 60 000, 30 mg) was added to the DMF solution (20 mL) of *N*-(4-azidobenzoyloxy) succinimide (8.4 mg) under stirring in ice. After reaction at 4 °C for 24 h under stirring, the solution was ultrafiltered (Millipore MoleCutII, filtration off below 10 kDa) and washed with two 5-mL portions of 1/2 DMF/H_2O and then with 5 mL of MilliQ water. The number of azidophenyl groups in the polymer was determined by ^{1}H NMR from the peak intensities of the azidophenyl protons at 7.0 ppm and those of the methylene and methylidyne protons of the polymer main chain at 1.3 and 2.5 ppm.

Alternate Pattern Grafting of Polyallylamine and Poly(acrylic acid) Microgels. A polystyrene plate (2 cm × 2 cm) was cut from a tissue culture polystyrene flask. The azidophenyl-derivatized polyallylamine was dissolved in water (200 μg/mL). The solution (100 μL) was placed on the polystyrene plate and air dried at room temperature in the dark. The plate was covered with a patterned photomask having a 100-μm-wide stripe network and irradiated with ultraviolet light at an intensity of 10^5 μJ/cm^2 from a distance of 15 cm for 60 s. After irradiation, the plate was immersed in dilute hydrochloric acid (pH 3.0) and sonicated to completely remove the unreacted polymer in the unirradiated areas. After complete washing, the plate was dried in air. A polyallylamine microgel having the same pattern as that of the photomask was grafted onto the polystyrene plate surface.

Subsequently, the azidophenyl-derivatized poly(acrylic acid) was dissolved in water (500 μg/mL), and the solution (100 μL) was placed on the polystyrene plate patterned with the polyallylamine microgel and air dried at room temperature. The plate was covered with the same photomask that was turned 90° from its position for the PAAm microgel. The plate was irradiated with ultraviolet light at an intensity of 10^5 μJ/cm^2 from a distance of 15 cm for 60 s. The irradiated plate was immersed in and rinsed with an alkaline solution (pH 10) and then sonicated to remove unreacted azidophenyl-derivatized poly(acrylic acid). A PAAc microgel having the same pattern as that of the photomask was grafted onto the polystyrene plate surface and was laid perpendicularly to the PAAm microgel stripes. The grid pattern of PAAm and PAAc microgel networks was prepared. A similar grid pattern of PAAc and PAAm microgel networks was also fabricated using the same process by changing the preparation order of the two microgels.

Observation by SPM. An SPA400 (SII NanoTechnology Inc.) equipped with an Olympus rectangular cantilever (OMCL-RC800PB-1) having a spring constant of 0.11 N/m in contact mode was used for the measurements. All of the SPM measurements were made at room temperature (23 °C). The polystyrene plate grafted with the grid pattern of the PAAm and PAAc microgel network was first immersed in an aqueous HCl solution of pH 1.66, and a 150 μm × 150 μm area of the network was observed by SPM. The solution was then changed to a phosphate buffer (pH 7.4) or aqueous NaOH solution (pH 10.89), and the same measurements were performed.

Results and Discussion

Two photoreactive polymers, azidophenyl-derivatized poly(acrylic acid) (AzPhPAAc) and azidophenyl-derivatized polyallylamine (AzPhPAAm), were synthesized by coupling poly(acrylic acid) (PAAc) and polyallylamine (PAAm) with azidoaniline or azidobenzoic acid, respectively. The percentages of carboxylic groups in the PAAc and the amino groups in the PAAm coupled with the azidophenyl groups were 6.2 and 8.6%, respectively.

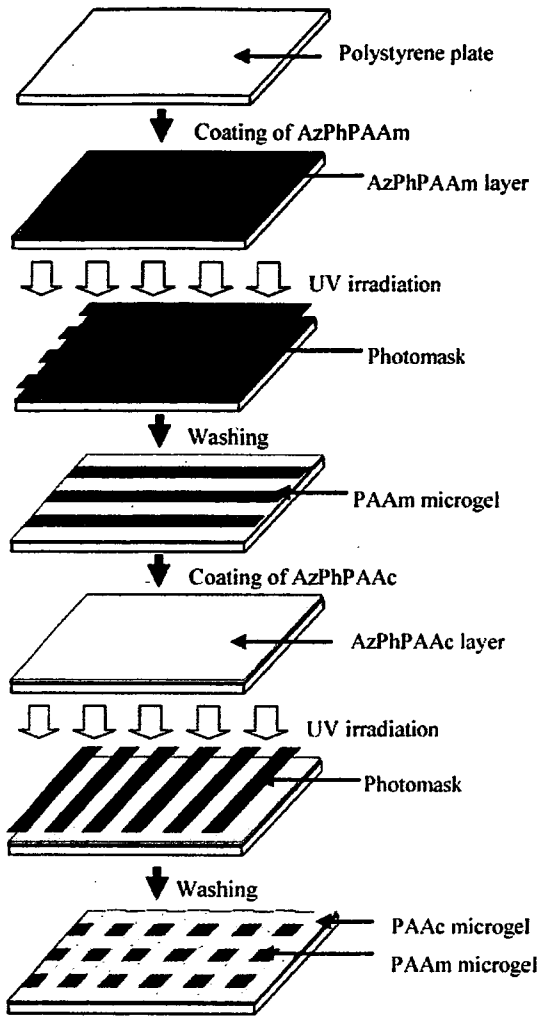

Figure 1. Photolithographic fabrication scheme of the grid pattern of microgel networks.

The preparation scheme of the grid pattern of microgels is shown in Figure 1. An aqueous solution of AzPhPAAm or AzPhPAAc was eluted on a polystyrene plate and air dried in the dark. The cast plate was photoirradiated in the presence of a photomask having a 100-μm-wide stripe pattern. AzPhPAAm or AzPhPAAc in the irradiated areas should be intermolecularly and intramolecularly crosslinked and grafted to the polystyrene surface. AzPhPAAm or AzPhPAAc in the other areas should not be crosslinked and could be removed by washing with an acidic or alkaline solution. After washing, a stripe network of a PAAm or PAAc microgel having the same pattern as that of the photomask was synthesized. Subsequently, a second microgel stripe pattern was grafted onto the first microgel. An aqueous solution of AzPhPAAc or AzPhPAAm was eluted onto the polystyrene plate grafted with the PAAm or PAAc microgel stripe pattern. The cast plate was photoirradiated in the presence of the same photomask that was turned 90° from the first pattern graft position. AzPhPAAc or AzPhPAAm in the irradiated areas should be intermolecularly and intramolecularly crosslinked and

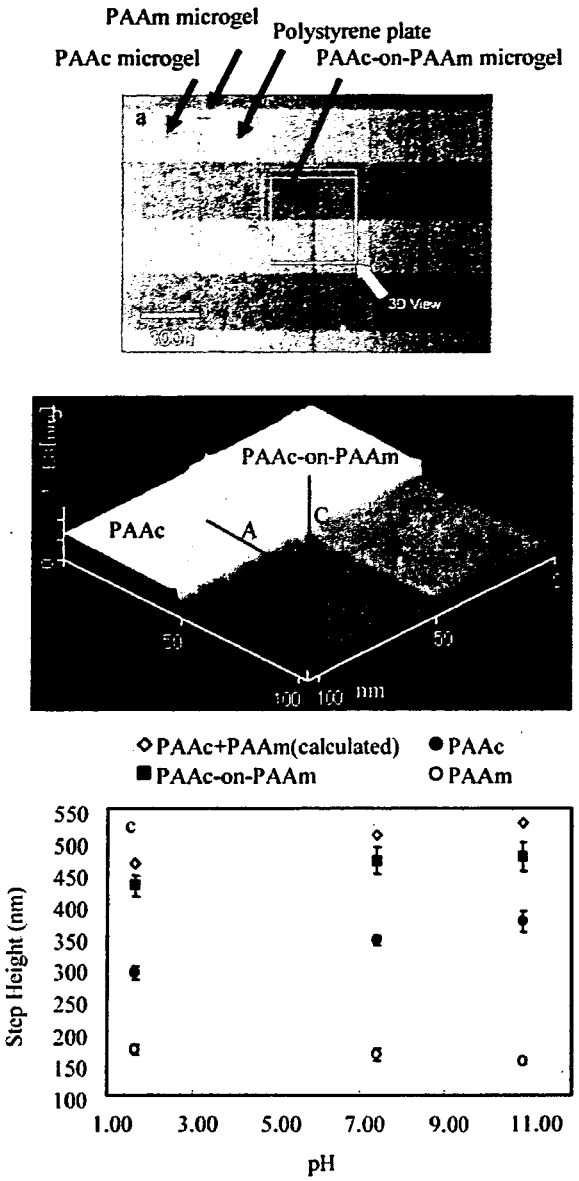

Figure 2. (a) Optical micrograph and (b) 3D topographic image of scanning probe microscopy (SPM) of a grid pattern of the PAAc-on-PAAm microgel network and (c) changes in the heights of the areas of PAAm, PAAc, and PAAc-PAAm microgels with changes in pH. The average value and the standard deviation for $n = 5$. The calculated height is the sum of the heights of PAAm and PAAc microgels.

grafted to the polystyrene surface and the first set of microgel stripes. AzPhPAAc or AzPhPAAm in the other areas should not be crosslinked and could be removed by washing with an acidic or alkaline solution. After washing, a grid pattern of a PAAc-on-PAAm or PAAm-on-PAAc microgel network was synthesized.

The grid pattern of PAAc-on-PAAm microgels was confirmed by optical microscopy (Figure 2a). The width of the microgel stripes and interstices was 100 μm. The swelling and shrinking behaviors of the PAAc-on-PAAm microgels were observed by SPM using contact mode. A 150 μm × 150 μm area was analyzed by changing the pH of the surrounding aqueous solution from 1.5 to 11.0. The terrace structure of the grid pattern of the PAAc-on-PAAm microgel at pH 10.89 was confirmed by a 3D image (Figure 2b). The areas of bare polystyrene, PAAc microgel, PAAm microgel, and PAAc-PAAm microgel had different heights and comprised the terrace structure. The step heights of the four areas were measured by scanning the adjacent areas along lines A−C. The thickness of the microgels was 140 to 500 nm and changed with the pH (Figure 2c). The height of the polystyrene area remained the same because polystyrene does not respond to changes in pH. The areas containing the PAAc, PAAm, and PAAc-PAAm microgels showed different swelling and shrinking properties when the pH was changed. The PAAc microgel swelled at high pH and shrank at low pH. The PAAm microgel swelled at low pH and shrank at high pH. However, the thickness of the joint areas did not change as significantly as those of the PAAc and PAAm microgel areas, indicating that the swelling and shrinking effects of the two microgels offset each other in the joint region. The pH-induced structure change was repeatedly reversible.

The pH responses of the PAAc, PAAm, and PAAc-PAAm microgels were demonstrated by SPM. Their swelling and shrinking can be interpreted as the result of the ionization and deionization of the carboxylic and amino groups in the PAAc, PAAm, and PAAc-PAAm microgel networks. For the PAAc area, the carboxy groups of the PAAc microgel network became ionized and the network swelled at pH 10.89 as a result of the repulsive interaction between negatively charged carboxylic groups. As the pH of the solution decreased, the ionized carboxylic groups became deionized, and hydrogen bonds between the carboxylic groups formed. As a result, the network shrank. However, for the PAAm area the situation was completely the opposite. The amino groups of the PAAm microgel network became ionized and the network swelled at pH 1.66 as a result of the repulsive interaction between positively charged carboxylic groups. As the pH of the solution increased, the ionized amino groups became deionized, and hydrogen bonds between the amino groups formed. Subsequently, the PAAm microgel area shrank. For the PAAc-PAAm microgel area, the response to pH is the sum as the effects from both the PAAc and PAAm microgels. At low pH, the amino groups of the PAAm microgel were ionized and swelled, and the carboxylic groups of the PAAc microgel deionized and shrank. At high pH, the carboxylic groups of the PAAc microgel were ionized and swelled, and the amino groups of the PAAm microgel became deionized and shrank. The opposite response of the PAAc and PAAm microgels partially counteracted the swelling and shrinking effects of each other in the joint area. However, the height of the joint area was not the simple sum of the heights of the PAAc and PAAm areas. It was lower in the range of 30 to 50 nm than the sum of the heights of the PAAc and PAAm areas. The reason might be that the interface of the PAAm and PAAc microgels in the joint area may not be a simple lamination of the two microgel sheets. The photoreactive polymer solution might penetrate the first microgel network in the joint area during the second patterning process. Therefore, the upper microgel might penetrate the microgel lying beneath it. The negatively charged carboxylic groups and positively charged amino groups might form ion complexes that result in the formation of a compact structure at the very thin interface and may not be a response to pH change. The compact interface structure thus decreased the total height of the overlapped area.

In recent years, microfabrication and micromachining techniques and nanotechnology have been widely used in various fields such as the integrated circuit industry, molecular electronics, biosensing, tissue engineering, and so forth. It would be interesting to apply polymer gels in such fields because polymer gels undergo abrupt changes in volume by swelling and shrinking in response to external stimuli. However, it has been difficult to control the

structure of microgels and to synthesize microgel networks. In the present study, photolithography was used to prepare a grid pattern of pH-sensitive nanothick microgels. The grid pattern constituted of four grids that had different responses to changes in pH. The nanothick microgels showed a rapid, reversible response to changes in pH. By using this technique, it would be possible to prepare nanothick microgel networks with both positional and functional patterns by using different stimuli-responsive polymers. These kinds of nanothick microgel networks would find wide applications in devices such as smart actuators, artificial muscles, sensors, and drug delivery systems as well as in tissue engineering and so forth.

Acknowledgment. This work was supported in part by the New Energy and Industrial Technology Development Organization of Japan and in part by the Ministry of Education, Culture, Sports, Science and Technology of Japan.

LA700931U

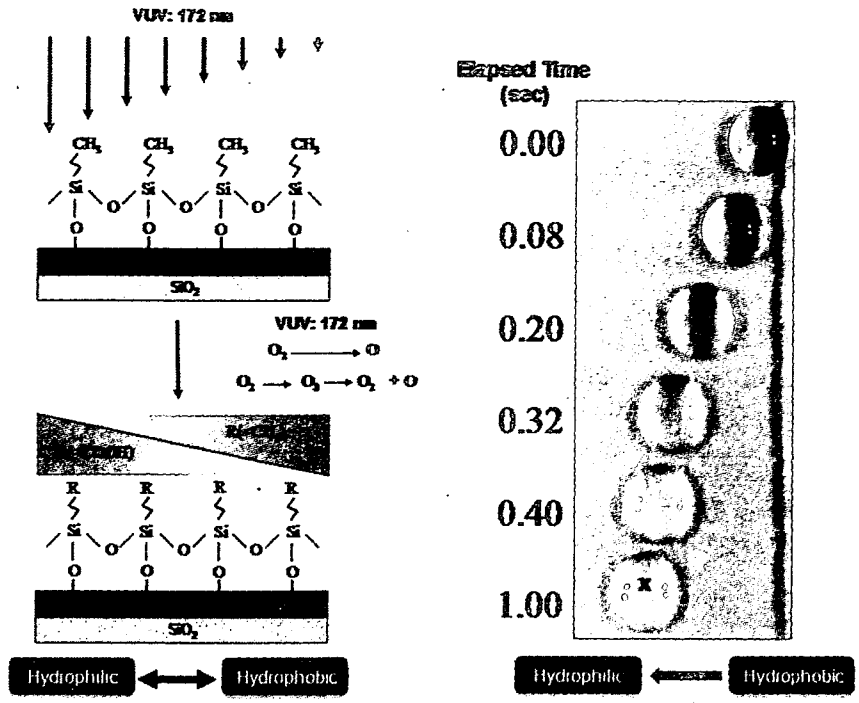

Control of Water Droplet Movement

Yoshihiro ITO
y-ito@riken.jp
Nano Med. Eng. Lab., RIKEN

A hydrophobic to hydrophilic gradient surface was prepared using the tuned photodegradation of an alkylsilane self-assembled monolayer (SAM) using irradiation of vacuum ultraviolet light (wavelength = 172 nm). The water contact angle on the photo-degraded SAM surface was adjusted using the intensity and time photo-irradiation parameters. The water drop moved from the hydrophobic to hydrophilic surface with a velocity that depended on the gradient. The higher the gradient, the faster the water moved. For the first time, we have prepared a gradient surface using photodegradation where the movement of a water drop was regulated by the degree of gradation.

Polymer Preprints, Japan **2007**, *56*, 1532.

総説（Review Article）：膜（MEMBRANE），32（5），276-280（2007）

●特集｜人工膜関連シンポジウム「膜を用いた新しい細胞培養操作」

再生医療のための幹細胞増幅基材

伊藤嘉浩

理化学研究所　伊藤ナノ医工学研究室　〒351-0198 埼玉県和光市広沢2-1

Biomaterials to *Ex Vivo* Expand Stem Cells for Regenerative Medicine

Yoshihiro Ito

Nano Medical Engineering Laboratory, RIKEN, 2-1 Hirosawa, Wako-shi, Saitama 351-0198, Japan

For achievement of regenerative medicine, *ex vivo* expansion of stem cells which can be differentiated to various cells is very important. However, it is very difficult to efficiently and safely culture some stem cells such as hematopoietic stem cells in cord blood or human embryonic stem cells. Therefore, the culture systems are investigated by many researchers. Here the state-of-arts of culture of stem cells and in particle development of biomaterials for expansion of stem cells is discussed.

Key words : cell culture／stem cell／biomaterial／immobilization／growth factor／nurse cell

1. はじめに

これまで半世紀にわたり，人類は病気で機能障害や機能不全に陥った生体組織・臓器の治療のために近代的な人工臓器や臓器移植を発展させてきた（Fig. 1）．しかし，人工臓器はまだまだ不備が多く，臓器移植ではドナーの不足が深刻である．そこで最近「再生医療」という細胞を積極的に利用して，生体機能の再生をはかる医療が考えられるようになった．再生医療は，1997年のクローン羊の出現や1998年のヒト胚性幹（ES）細胞の樹立から注目を集めるようになった．再生医療では，ES細胞ばかりでなく，成人の体のなかにも体性幹細胞が存在することがわかり，一部はすでに医療に用いられ，今後その治療用途はますます拡大してゆくと考えられている（Fig. 2）．このような医療の実現のための一つの大きな課題は，非常に僅かしかない幹細胞を未分化状態のまま効率よく増やすことである[1~9]．

我々は，これまで成長因子やサイトカイン固定化材料が細胞培養に応用できることを示してきた[10~14]．もしこのような基材を用いて，再生医療で重要となるヒト幹細胞を，安全かつ迅速に供給できるようにするバイオリアクターが開発できればと考えた．これまで，生体外での細胞培養は長い歴史をもち，この技術により生命科学は飛躍的な進歩を遂げてきた．今や実験手段として細胞培養は日常的で不可欠な技術になっているが，通常は，動物から採取した血清を用い，場合によっては異種動物由来の細胞を培養液に共存させて行われている．しかし，ヒト幹細胞を培養し，医療に用いるためには，安全な培養が最も重要である．異種動物由来の血清や細胞の使用は，これまでしばしば指摘され問題になってきたようにウイルスやプリオン感染，さらに未知の病原体による感染を招く恐れがある．そこで，これら異種動物由来の生体成分を混在させない完全な人工幹細胞培養系を確立することが必須となる．

2. 化学固定化保育細胞による培養システムの開発

白血病治療は，骨髄移植，末梢血幹細胞移植から，

Tel : 048-467-5809　Fax : 048-467-9300
E-mail : y-ito@riken.jp

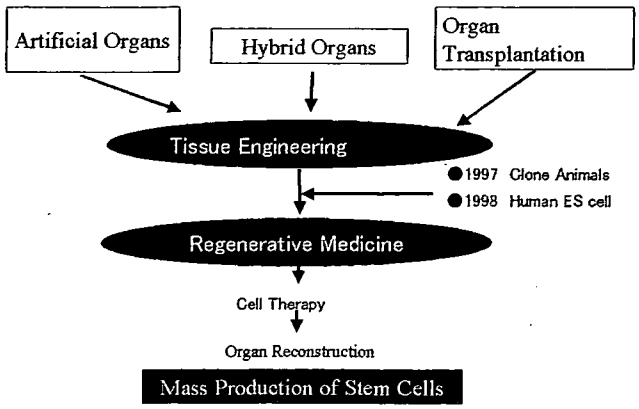

Fig. 1 History to regenerative medicine.

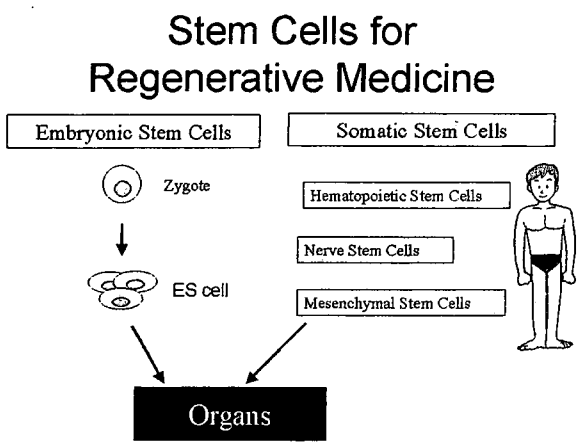

Fig. 2 Stem cells for regenerative medicine.

臍帯血移植へと展開されてきた．臍帯血は，これまで廃棄されていたものを使用できる上に，組織適合性が寛容で冷凍保存も可能で今後の発展が期待されている．しかし一般に採取可能な臍帯血からは充分量の造血幹細胞が得られず，成人の治療には困難が伴っている．また，ヒトES細胞培養で動物由来血清や保育細胞を使用している場合，ヒト型でない化学修飾が起きるという報告が近年明らかにされた．そのため，これら幹細胞を異種動物由来成分を含まずに培養することが，望まれる．

我々は，まず国立がんセンターとの共同研究で，ヒト骨髄間葉系幹細胞（hMSC）の不死化をヒトテロメラーゼ逆転写酵素（hTERT）遺伝子導入により行い，これを保育細胞として用いた（Fig. 3）．不死化により株化細胞のようにhMSCが扱いやすくなった．さらに，不死化hMSCをアルデヒド基をもつ化合物で架橋固定化してもヒト臍帯血造血幹細胞の増幅支持能があることがわかった．特にグルタルアルデヒドで固定化した保育細胞は高い活性があり，長期的に冷蔵保存可能であることがわかった．さらには凍

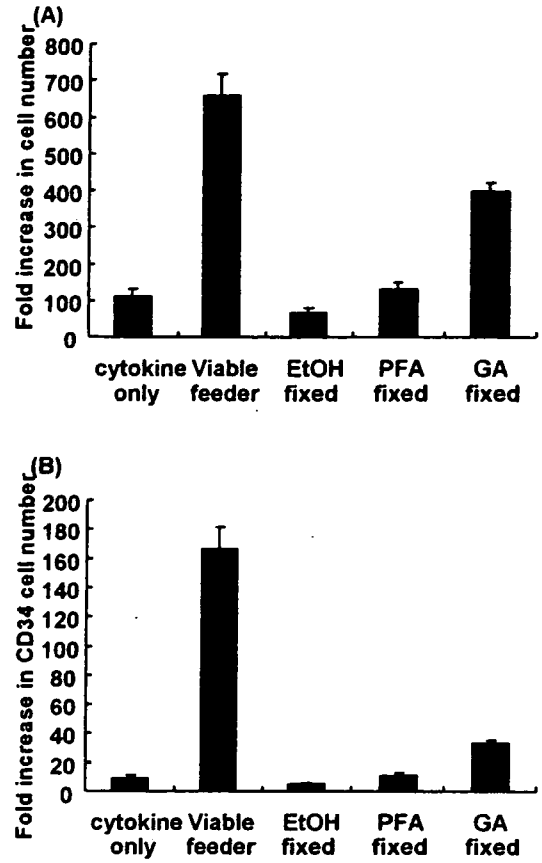

Fig. 3 *Ex vivo* expansion of (A) total cells and (B) $CD34^+$ (hematopoietic stem) cells in human cord blood. EtOH, PFA, and GA mean ethanol, paraformaldehyde, and glutaraldehyde, respectively. Viable feeder means non-fixed nurse cell.

結乾燥して保存しても，未分化状態の造血幹細胞の体外増幅支持に活性があることもわかった．凍結乾燥しても活性を保持できることから，保存性の高い利用しやすい基材とすることができた[15]．

一方，霊長類ES細胞培養のためには，医療廃棄物として捨てられる胎盤からヒト羊膜上皮細胞を採取し，保育細胞となることを見出した[16]．これについても国立がんセンターとの共同研究でhTERT導入により不死化し，その上で化学固定して培養用基材とする検討を行った．その結果，グルタルアルデヒドやホルムアルデヒドで固定化した不死化ヒト羊膜上皮細胞も，サルES細胞の未分化状態での増殖を支持することがわかった（Fig. 4）．さらに，化学固定化細胞はそのまま凍結乾燥保存できることや，一旦培養に用いた化学固定化細胞は，培養したES細胞をトリプシン処理して剥がしてから再度利用できることもわかった[17]．通常，保育細胞は，培養したい細胞の培養の時期にあわせて培養する必要があり，手間がかかったが，本研究のような化学固定化細胞を用

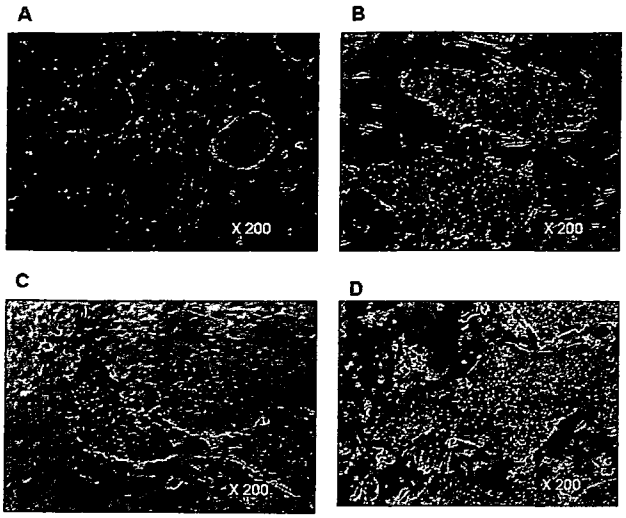

Fig. 4 Monkey embryonic stem (ES) cells on (A) primary mouse embryonic fibroblast treated with mitomycine-C, (B) human amniotic epithelial cells treated with 2.5% glutaraldehyde, (C) human amniotic epithelial cells treated with 2.5% formaline, and (D) coated gelatin were cultured, and they were stained with alkali phosphatase activity. On (A), (B), and (C) the monkey ES cells were stained but not on (D). This result indicated that ES cells grew with undifferentiated state on (A), (B), and (C).

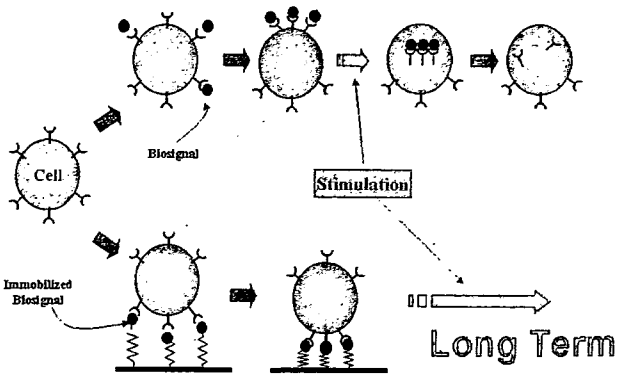

Fig. 5 Interactions of a soluble (above) and an immobilized (below) biosignal molecule. When a soluble biosignal molecule interacts with the cognate receptor, a complex is formed and the complexes are aggregated on the cell membrane. Subsequently the complexes are internalized and decomposed in the cell. The final process is called down-regulation and the mechanism contributes the reduction of overloading of stimulation by decreasing the number of receptors on the cell membrane. If the biosignal molecule is immobilized on materials, this down-regulation process is considered to be inhibited and stimulation will continue for a long time.

いれば，そのような手間が省け，有用と考えられる．

3. 成長因子固定化材料の開発

再生医療では，幹細胞と，成長因子，そしてマトリックスが重要な因子となることが知られている．我々は，成長因子とマトリックスを組み合わせた新しい再生医療材料の開発を長年行ってきた．その主たる方法は，化学的手法によるもので，1990年代前半は，材料表面にカルボキシル基のような官能基を提示させ，そこに成長因子を固定化する手法を主に用いてきたが，1990年代後半からは，光リソグラフィ法による固定化を主に用いるようになった．これは特定の官能基を必要としないこと，マイクロパターン状固定化が簡単に行え，固定化成長因子の作用を顕微鏡下で視覚的に容易に観測できることから採用した．そして，インシュリン，上皮細胞成長因子（EGF），神経細胞成長因子（NGF），血管内皮細胞成長因子（VEGF）[18]などを固定化し，固定化領域で細胞成長や分化を制御できることを見出すとともに，固定化成長因子は細胞内に取り込まれずにダウン・レギュレーションを抑制し，刺激効果が高いことを明らかにしてきた（Fig. 5）．最近では，この他にも

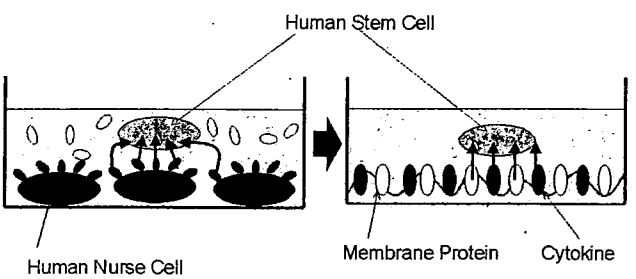

Fig. 6 Culture of human stem cells not in the presence of human nurse cells but on artificial protein layer composed of membrane proteins of nurse cells and cytokines in culture medium is desirable for future.

様々な成長因子が固定化され，その効果が実証されるようになってきている[14]．

上述の化学固定化保育細胞が幹細胞増幅活性をもつことから，Fig. 6に示すように保育細胞の膜タンパク質を固定化すれば同等の効果をもつ完全な人工膜を作出でき，より安全性が高く大量生産可能になると考えられる．そこで，いくつかのタンパク質固定化材料を新たに調製して造血幹細胞あるいはそのモデルとなる血球系細胞の培養を行い，その効果を検討した．その中で，エリスロポエチンをマイクロパターン状に固定化した材料を作成し，その上でUT7-

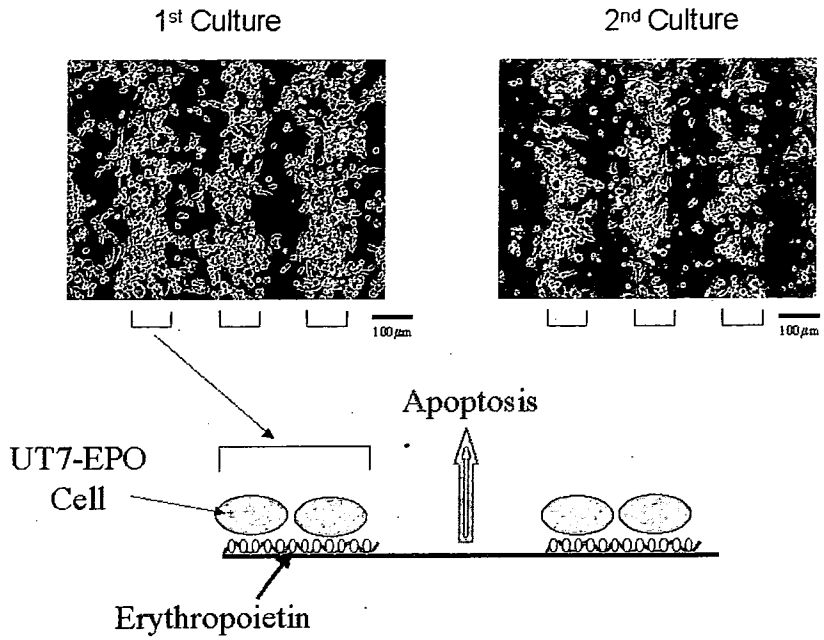

Fig. 7 Culture of erythropoietin-dependent UT7 (UT7-EPO) cells on erythropoietin-micropattern-immobilized surface. Although apoptosis was induced on the cells on non-immobilized surface, the cells on immobilized surface survived. In addition, the micropattern-immobilized surface can be used for second culture of cells.

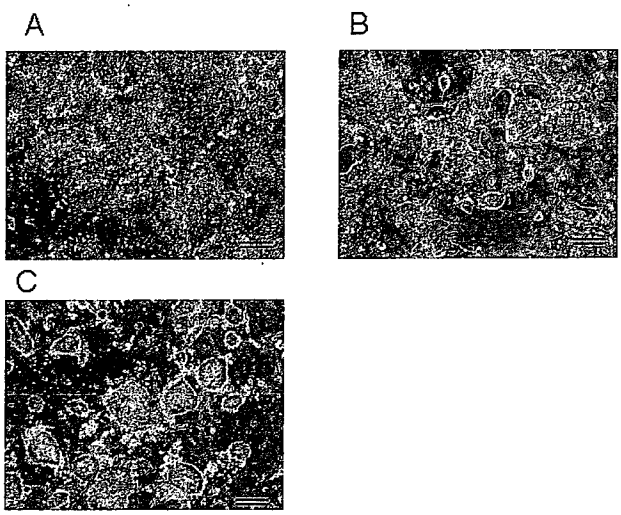

Fig. 8 Culture of mouse embryonic stem (ES) cells (A) in the absence of leukemia inhibitory factor (LIF), (B) in the presence of soluble LIF, and (C) in the presence of immobilized LIF and stained with alkali phosphatase activity. Although in (A) the cells were not so stained, in (B) and (C) the cells were stained. This result indicates that LIF was active for keeping undifferentiated growth of mouse ES cells in the soluble and immobilized states. Bars represent 200 μ m.

EPO細胞（エリスロポエチン依存性白血病細胞）を培養すると固定化領域でだけ細胞の増殖が観測され，非固定化領域ではアポトーシスが誘導される結果となり，固定化サイトカインの有効性を示すことができた（Fig. 7）[19]．また，造血幹細胞増幅と同様，ES細胞培養用にタンパク質の固定化による培養基材の開発を目指した研究も行った．マウスES細胞の培養のためには白血病抑制因子（LIF）と呼ばれるタンパク質を培養液に添加して未分化状態を保持することが行われるが，これを固定化しても活性を保持することを見出した（Fig. 8）[20]．

4. 課題及び今後の展望

保育細胞を化学固定化して基材として実際の幹細胞の増幅促進までは行うことができたが，タンパク質の固定化だけでは，実際の幹細胞の増殖促進までには至っていない．これは，幹細胞のニッチェ（周辺環境）に関する科学がまだ十分に理解されておらず，工学的にアプローチできる手段や分子情報が限られていることによる．そのため，幹細胞増幅活性をもつ保育細胞から膜タンパク質を探索することが必要である．再生医療の発展のために切実に望まれる技術であることから，今後も生命科学研究者との連携をさらに密にして展開することが重要である．

謝　辞

本研究は，財団法人神奈川科学技術アカデミーの

伊藤「再生医療バイオリアクター」プロジェクトの研究の一環として行われた．財団からの物心両面からの援助に感謝します．

文　献

1) 伊藤嘉浩：分子細胞療法, **2**, 52-55 (2003)
2) 伊藤嘉浩：工業材料, **52**, 12-13 (2004)
3) 伊藤嘉浩：表面科学, **25**, 16-22 (2004)
4) 伊藤嘉浩，金野智浩，宮本寛治：バイオインダストリー, **21**, 5-11 (2004)
5) 伊藤嘉浩, 野川誠之, 金野智浩, 牧野　弘, 蓮田寛和, 宮本寛治, 池淵研二：再生医療学会誌, **3**, 55-61 (2004)
6) 伊藤嘉浩：*Organ Biology*, **12**, 47-55 (2005)
7) 伊藤嘉浩：未来材料, **5**, 46-47 (2005)
8) 伊藤嘉浩：「図解高分子新素材のすべて」，国武豊喜監修, 工業調査会, pp. 94-97 (2005)
9) 伊藤嘉浩：化学, **62**, 38-41 (2007)
10) 伊藤嘉浩：「高分子材料・技術総覧」，高分子材料・技術総覧編集委員会, 産業技術サービスセンター, pp.615-622 (2004)
11) 野川誠之, 伊藤嘉浩：遺伝子医学 Mook, **1**, 88-93 (2004)
12) 北嶋　隆, 伊藤嘉浩：再生医療学会誌, **4**, 53-61 (2005)
13) 伊藤嘉浩：「再生医療」，田畑泰彦, 赤池敏宏編集, コロナ社, pp.221-235 (2006)
14) Ito Y : *Soft Matter*, in press (2007)
15) Ito Y, Hasuda H, Kitajima T, Kiyono T : *J. Biosci. Bioeng.*, **102**, 467-469 (2006)
16) Miyamoto K, Hayashi K, Suzuki T, Ichihara S, Yamada T, Kano Y, Yamabe T, Ito Y : *Stem Cells*, **22**, 433-440 (2004)
17) Ito Y, Kawamorita M, Yamabe T, Kiyono T, Miyamoto K : *J. Biosci. Bioeng.*, **103**, 113-121 (2007)
18) Ito Y, Hasuda H, Terada H, Kitajima T : *J. Biomed. Mater. Res.*, **74**, 659-665 (2005)
19) Ito Y, Hasuda H, Yamauchi T, Komatsu N, Ikebuchi K : *Biomaterials*, **25**, 2293-2298 (2004)
20) Makino H, Hasuda H, Ito Y : *J. Biosci. Bioeng.*, **98**, 374-379 (2004)

(Received 22 June 2007;
Accepted 10 July 2007)

著者略歴

伊藤　嘉浩（いとう　よしひろ）

1981年3月　京都大学工学部高分子化学科卒業
1986年3月　同大学大学院工学研究科研究指導認定退学
1987年1月　同大学工学博士
1988年4月　同大学　助手
1996年2月　同大学大学院　助教授
1997年4月　奈良先端科学技術大学院大学　助教授
1999年4月　徳島大学　教授
2002年4月　神奈川科学技術アカデミー　プロジェクトリーダー
2004年5月　理化学研究所　主任研究員

幹細胞培養のための ナノ界面創成バイオリアクター

伊藤嘉浩（いとう よしひろ）
（独）理化学研究所伊藤ナノ医工学研究室

再生医療の話題は，科学を超えて事欠かない．2004年のアメリカ大統領選では，胚性幹（ES）細胞の研究が争点の一つになり，結局，ヒトES細胞研究に消極的なブッシュ大統領が勝利した．しかしその後，シュワルツェネッガー知事のカリフォルニア州では，住民投票による賛成多数の支持を受け，ヒトES細胞研究を中心とした再生医療の基礎研究に対し，今後10年間で州予算から約30億ドルを出資することになった．また，2005年末から2006年はじめにかけては，韓国でのクローン化ヒトES細胞のねつ造問題が世界中の注目の的となった．

「夢の医療」として再生医療が注目を集めるようになった経緯を図1に示す．もともと，病気で機能障害や機能不全に陥った生体組織・臓器の治療のために，近代的な人工臓器や臓器移植が発展してきた．しかし，人工臓器の高性能化には現在のところ限界があり，臓器移植ではドナーの不足が深刻である．日本で脳死移植が可能となった1997年の臓器移植法の施行以来，現在までの移植件数は50件ほどにとどまっている．そのようななか，1980年代後半からハイブリッド人工臓器の先駆けとなった培養皮膚の考えを発展させた「生体組織工学（tissue engineering）」という概念が生まれた．これは，生分解性マトリックスを足場にして生体内外で組織再生を行わせようとするものであった．そして1990年代後半になると，クローン技術の発明（クローン羊の誕生）と，ヒトES細胞の樹立という二つの大きな進展により「再生医療」という，幹細胞を積極的に利用して生体機能の再生を図る医療が考えられるようになった[1]．

再生医療のための幹細胞

再生医療への期待が膨らんだ背景には，ヒトES細胞の樹立以外に，成人体内でも多くの幹細胞が存在することが明らかになってきたからである．幹細胞とは，さまざまな細胞へ

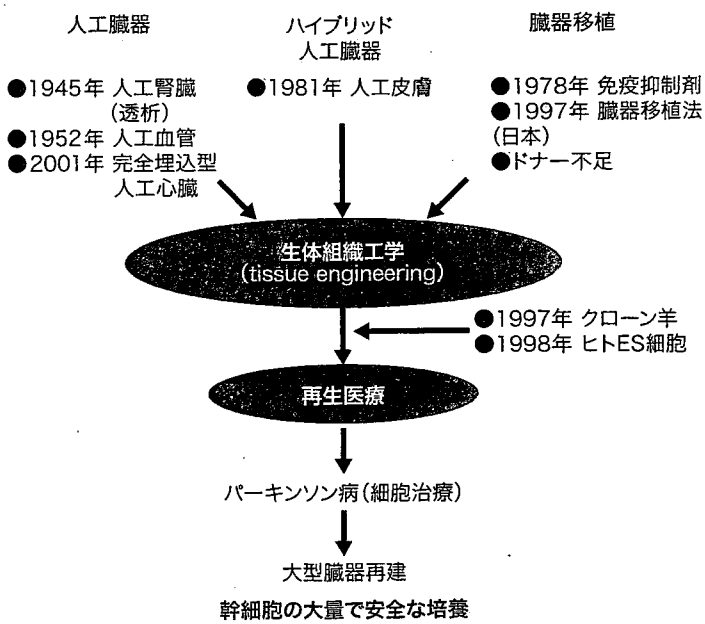

図1　再生医療研究への流れ

伊藤嘉浩（いとう よしひろ）
＜所属＞（独）理化学研究所主任研究員（伊藤ナノ医工学研究室），＜出身大学＞京都大学（1981年卒業），＜研究テーマ＞再生医療工学，コンビナトリアルバイオエンジニアリング，ソフトナノテクノロジー，＜趣味＞そぞろ歩き

分化できる能力をもったまま未分化の状態で自己複製できる細胞であり，受精卵からつくる上述のES細胞と成人にも存在する体性幹細胞の二つに分類される（図2）．前者は，今や世界各国で樹立されてきてはいるものの，まだ倫理的な問題や多くの技術的な問題があり，医療への応用実現には多くの年月が必要と思われている．一方，後者については着実に医療として定着しはじめている．

臓器や細胞を用いる移植医療には，自家移植と同種（他家）移植がある．自家移植とは，患者自身の組織を移植するものであり，形成外科や整形外科の医療機関内で皮膚や骨の異所への移植は比較的古くから行われている．再生医療では，患者自身の幹細胞を本来のものとは異なる臓器部位に移植する．たとえば，骨髄中の間葉系幹細胞がさまざまな細胞に分化できることがわかり，さまざまな臓器の再生に用いられるようになってきた．日本では，閉塞性動脈硬化症やバージャー病など虚血下肢治療のために患者自身の骨髄細胞を用いる方法がはじめて一部保険適用できる「（高度）先進医療」として2003年に認可を受けた．現在，骨髄細胞を歯周病治療，心疾患，脳疾患（脳梗塞），脊髄損傷などへ治療応用する研究がさかんに行われている．骨髄細胞以外にも，血液からの幹細胞で急性心筋梗塞患者の治療を行った例や，患者自身の口の粘膜の細胞を使って目の角膜を再生する臨床試験の成功が報告されている．そのほか成人の鼻粘膜細胞を用いた脊髄損傷治療や，患者の太ももから筋肉の一部を用いた疾患治療が行われている．また，脂肪吸引でとった脂肪組織中の幹細胞も細胞ソースとして有用であり，臨床応用が試みられている．

一方，同種移植では，ドナーからの直接の臓器移植に加えて，冷凍保存した臍帯血（臍の緒のなかに含まれる血液）のなかにある造血幹細胞を用いた治療も一般的治療として行われている．臍帯血は，これまで廃棄されていたものを使用できるうえにドナーへの負担がなく，組織適合性が寛容で冷凍保存も可能という利点がある．現在，日本には全国に11の公的な臍帯血バンクがあり，白血病などの血液疾患の治療に用いられている．同種移植が広く可能になれば，大きな福音となることは確かである．

幹細胞の体外増幅のためのバイオリアクター

このように再生医療は着実に進展している．しかし，再生医療の大きな進展を阻むものの一つとして，幹細胞の存在量の少なさがある．そこで，これを補うために幹細胞を体外増幅する培養用バイオリアクターが研究されてきている．免疫療法では，がんを攻撃する免疫細胞を患者自身から採取し，体外増幅して体内へもどす治療が行われている．もし，さまざまな細胞を安全に体外増幅させる技術が確立できれば，再生医療をはじめさまざまな医療への応用展開が可能となる．

とくに，さかんに研究されているのが，臍帯血の造血幹細

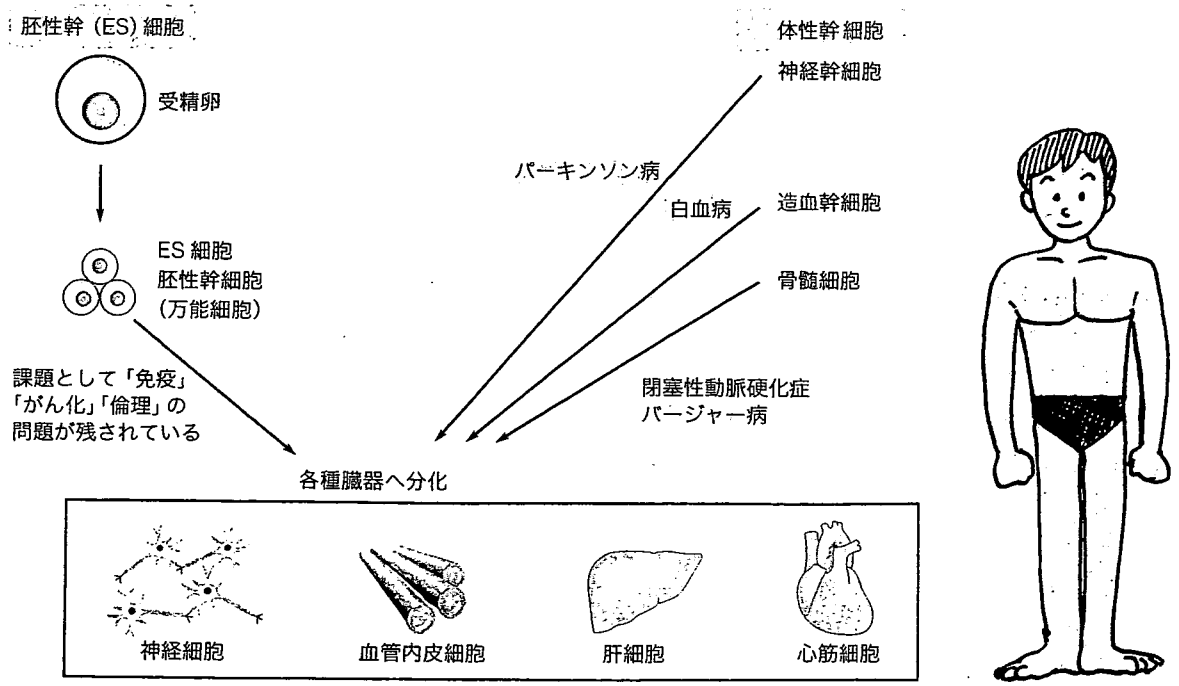

図2　再生医療のためのES細胞と体性幹細胞